Automatic characterisation of chars from the combustion of pulverised coals using machine vision

Deisy Chaves[a,*], Laura Fernández-Robles[b], Jose Bernal[c], Enrique Alegre[b], Maria Trujillo[a]

[a] *Multimedia and Computer Vision group, School of Computer and Systems Engineering, University of Valle, Ciudad Universitaria Meléndez, Cali, Colombia*
[b] *School of Industrial and Informatics Engineering, Universidad de León, Campus de Vegazana, Leon 24071, Spain*
[c] *Computer Vision and Robotics Institute, Department of Computer Architecture and Technology, Universitat de Girona, Girona 17003, Spain*

Abstract

The study of char morphology, produced during combustion of pulverised coal, may be used to evaluate the effect of coal on the performance of the burner. Particle reactivity is the response to temperature and oxygen concentration and depends on particle size and other variations during the combustion. In this paper, we automatically characterised chars from the combustion of pulverised coal using machine vision. We have followed two different approaches to describe the chars: (i) its morphology and (ii) its intensity distribution provided by texture features. We realised that each of the binary layers obtained after bit-plane slicing a char image returned different representations that highlighted either rough or fine details. Hence we combined this finding with the two previous characterisation approaches. Thus, in this paper, we described char images using both morphology and texture computed on some specific bit-plane slices, and later on, we automatically classify each particle based on its description as having high, medium or low reactivity. To validate experimentally the proposed method we used char images from coals of three Colombian regions: Valle, Antioquia and Cundinamarca. We determined the reactivity of a coal sample by

*Corresponding author. Address: Multimedia and Computer Vision group, School of Computer and Systems Engineering, University of Valle, Ciudad Universitaria Meléndez, Calle 13 No. 100-00, Cali, Colombia. Tel:+57 2 321 21 00
Email address: deisy.chaves@correounivalle.edu.co (Deisy Chaves)

calculating the percentage of particles assigned to each of the three previous reactivity groups. The method that we are proposing obtains similar precision to the obtained by the manual analysis of char morphology following the International Committee for Coal and Organic Petrology criteria, but with the advantages of analysing the particles reactivity automatically.

Keywords: Char morphology, coal combustion, coal reactivity, image processing, machine vision

1. Introduction

The pulverised coal combustion is a technology extensively used to generate electricity. Char particles with distinctive morphologies are produced during the first stage of the combustion process or devolatilisation. Char morphology depends on coal composition —e.g. coal type and coal rank— and is affected by the combustion parameters —e.g. residence time and temperature [1, 2]. The knowledge of the specific char morphology may be used to determine coal reactivity and combustion performance in power plants. In fact, coals generating char particles with high porosity and thinner walls are more reactive and desired for combustion. Moreover, the optimal selection of boiler parameters increases combustion efficiency and reduces the release of CO_2, ash and other residues to the environment [3, 4].

Char morphology has been widely studied by the Combustion Working Group in Commission III of the International Committee for Coal and Organic Petrology (ICCP) which published a classification contemplating nine char types [5, 6], it is registered in Table 1. We considered the first eight char types, in order of appearance on the table, to summarise them into three groups of char morphologies based on porosity, wall thickness and shape of particles. Porosity to represent the chemical reaction of oxygen with the internal surface of the particle, wall thickness to represent the extent of this surface, and shape to describe the degree to which oxygen diffusion through the pores restricts the reaction. As a result, three groups of char morphologies are: (i) *High reactive* characterised by thin-walled, high porosity and sizeable superficial area —i.e. TS, TN, CS, CN char types; (ii) *Medium reactive* identified by pore-dense mixture with pore or dense part predominance —i.e. MP and MD char types; and (iii) *Low reactive* described by thick-walled, low porosity and small superficial area —i.e. I and S char types. The mineroid char type identification requires quantification of mineral matter which employs several techniques such as Rietveld-based X-ray powder diffractometry, computer-controlled scanning electron microscopy and fluorescence microscopy analysis. These processes were considered out of the scope of this research as they increase cost and study time.

Commonly, char characterisation is manually done using an electronic microscope to analyse a char-block —i.e. mix of resin and chars from a coal sample [1]. Wu et al. [7] recommended the analysis of 500 char particles to guarantee reproducibility of results. Following this recommendation, at least 500 char particles are looked on the surface of a char block through a microscope and classified according to the morphological characteristics defined by the ICCP's classification [8, 5, 6]. Frequencies of each char type are used to define the reactivity of char samples. The char type with the highest rate is adopted as an estimation of the coal reactivity. Naturally, this process may be subjective, error-prone and requires a significant amount of time when carried out manually [3].

Nowadays, image processing is becoming an alternative way to automate manual analysis by creating accurate and low-cost tools. Some systems relying on machine vision for coal characterisation comprise classifying coal quality into three fixed categories —best, good and poor— based on texture and colour features [9], predicted coal ash content [10], or estimated particle size and its distribution on fine coal [11], among others. Similarly, the analysis and classification of char particles can be carried out automatically by applying machine vision techniques on: (i) digital images taken from a char-block using a microscope [12, 13, 7, 14, 15] and (ii) high-speed videos of char particles during combustion [16, 17, 18].

Char digital images are processed to identify particles and to calculate features which describe them automatically. This set of features is used to build a classification model and automatically assign the analysed particles to a char type —i.e. ICCP char types— or a char group —i.e. high, medium and low reactive. In [12, 13, 7, 14, 19] morphological features such as porosity, unfused material, wall thickness and sphericity are used to classify particles into char types following the ICCP criteria. In [19] besides morphological characteristics, local features are used to represent two groups of char morphology particles: (i) high reactive —i.e. TS, CS, TN, CN char types— and (ii) low reactive —i.e. MD, MP, S, I char types. Features obtained from a set of manually annotated char images are utilised to build a char classifier employing Support Vector Machine (SVM) and Random Forest algorithms. Naturally, the advantage of such automatic approaches to classify chars over the ICCP manual characterisation is the ability to analyse larger and varied coal samples. This asset is desirable as coal samples with different compositions from the ones used to build the ICCP characterisation may not fit into it. For instance, the ICCP characterisation does not produce accurate results on Colombian coals since the primary decision variable, unfused material, is scarcely seen in Colombian char samples due to the low amount the inertinite material present in them [2, 20].

High-speed video analysis is used to develop applications for detecting changes in particle size and shape during coal combustion [16] and mix of coal and biomass [17, 18]. They use a special arrange of cameras and combustion equipment to track and record the changes in temperature, velocity, area and perimeter of the char particles during the combustion with the aim to understand better the particle behaviour in this process. Particles are identified in each frame using threshold values set manually. We focus on the analysis of char images taken from a char-block using a camera attached to a microscope. These cross-section images are intended to quantify morphological features such as porosity and wall thickness that are commonly used to describe particles.

In this paper, automatic char characterisations are built using both supervised learning algorithms —SVM and deep learning. Global features —porosity, sphericity, and wall thickness— and local visual descriptors [21] —Local Binary Pattern (LBP) [22], Complete Local Oriented Statistical Information Booster

(CLOSIB) [23], Histogram of Oriented Gradient (HOG) [24], Scale-Invariant Feature Transform (SIFT) [25]— are used to describe particles. Features are obtained from char images and eight one-bit plane slices composing them [26]. Image slices emphasise relevant details that seek a better image representation and improve char classification. This kind of image analysis was successfully used in other problem domains such as natural image classification [27, 28] and face recognition [29]. To the best of our knowledge, this is the first time that bit-plane slicing analysis is applied to char morphology characterisation. The proposed char characterisation is validated by experiments using char images obtained from coals of three Colombian regions: Valle, Antioquia and Cundinamarca. Results show that our proposal accurately characterises particles using the considered char groups and, therefore, the reactivity of a given coal sample.

2. Materials and methods

We propose a system to characterise a coal sample based on char classification which is five-fold, as shown in Fig. 1. Firstly, a set of 120 images are obtained from a char-block using a microscope with an attached camera. Regions of the images that contain individual char particles are cropped from the captured images. Secondly, cropped images are processed to remove the background and to obtain eight bit-plane slice images. Thirdly, the content of particle images and bit-plane slice images are represented either by measuring morphological features, called global features, or calculating local texture and local shape, called local features. Global features correspond to eight morphological features chosen using the ICCP criteria —area, devolatilised material, undevolatilised material, number of pores, porosity, sphericity, and wall thickness. Local features —LBP, CLOSIB, HOG, SIFT— highlight visual patterns which are relevant to distinguish among char groups. The extracted features are concatenated to obtain a final representation of a char image. Fourthly, feature vectors are classified using a supervised learning algorithm. The classifier assigns each analysed char particle into one of the three char morphology groups

—high, medium or low reactive. Fifthly, the percentage of particles per group is computed to decide the final classification of a coal sample. The classification is based on 500 particles taking into account the findings of Wu et al. [7]. They proved that this amount of particles ensure reproducibility for char classification. The coal is characterised by the morphology of the group with the larger number of particles as high, medium or low reactive.

In this work, SVM and deep learning classification algorithms are evaluated. It is important to clarify that both strategies consider bit-plane slicing, but the former goes through all the steps aforementioned, while the latter does not as deep learning approaches compute their own features.

2.1. Char sample preparation and image acquisition

Coals from three Colombian regions —Valle, Antioquia and Cundinamarca— were used to generate char particles in a drop tube furnace (see Fig. 2), in a similar way to the reported in [13, 7, 30, 2]. The furnace was fed with coals of particle size of $-75\mu m$ and a nitrogen-oxygen mixture. Oxygen, $1\%v/v$, was used for facilitating tar oxidation and avoiding condensation. We set coal particle residence times, in the furnace, at $100ms$, $200ms$, $300ms$ with $800°C$, $900°C$, $1000°C$ using $104°C/s$ heating velocity. Parameters were set taking into account that (i) a system should be provided with different coals under assorted conditions to be robust and generalise well and (ii) settings should agree with average operating conditions used in industrial pulverised coal combustion plants.

Once chars were generated, the standard procedure to form char-blocks was followed [13, 7, 2]. First, char-blocks were created by mixing char samples, resin and liquid hardener. Second, each char-block surface was polished with fine polishing clothes using suspensions of alumina 0.5, 0.3 and 0.05 microns. Finally, a set of 120 digital images of 1600×1200 pixels were taken with a camera coupled to a metallographic microscope and 50X magnification lens, each image contained ten char particles in average (see Fig. 3). Individual particles were cropped from the captured images and manually labelled by experts in order to evaluate the performance of the automatic system.

2.2. Preprocessing

Preprocessing comprises two steps: background removal and data preparation. The former step involves removing char-block resin which is meaningless for our research. The background is identified and removed by applying a threshold method, called the Triangle method [31]. This method assumes a bimodal histogram of the grey levels of images, which char images satisfy, as shown in Figure 4. Two peaks can be observed in the histogram, the most prominent peak corresponds to the background pixels, and the smallest peak corresponds to the particle pixels. Briefly, the Triangle method draws a line between the maximum value of the histogram and the lowest value larger than zero. The threshold is set to the value that maximises the distance between the histogram and the line. The value of the threshold depends on the content of the image and is different and automatically calculated for each analysed image (see Fig. 4). All the intensities above the obtained threshold are considered as background and those pixel values set to zero. The latter step consists of extracting bit-planes using the slicing method [26]. As each grey intensity value is represented by eight bits, an image can be seen as a stack of eight one-bit plane slices or binary images, ranging from bit-plane slice zero for the least significant bit to bit-plane slice seven for the most significant bit (see Fig. 5). This approach highlights the contribution made to char image appearance by specific bits. Therefore, the lower order slices contribute more to fine (often imperceptible) visual details of char particles while the higher order slices contain a significant amount of relevant information.

2.3. Feature extraction

Global and local features are used to describe the image content and the eight composing slices. Global ones correspond to nine morphological features based on ICCP criteria [19]: area, devolatilised material, undevolatilised material, number of pores, porosity, sphericity and wall thickness, described in Table 2. Feature vectors are normalised to avoid using different scales.

Local features —LBP, CLOSIB, HOG, SIFT— highlight visual patterns or texture information which are relevant to distinguish chars groups. LBP [22] searches for binary texture patterns at each pixel considering a circular region. The LBP was computed using a radius of three and considering eight neighbours. HMCLOSIB [23] calculates statistical information of the gradient magnitude of image pixels considering a circular region at different scales. The HMCLOSIB was computed considering 16 neighbours with radii of 2, 3 and 4, and statistical measures of order 1 and 2. HOG [24] creates histograms by counting the frequency of gradient angles in an image. HOG was calculated considering eight angles. SIFT [25] computes a histogram of the gradient orientation, in a small image patch. We use a Bag-of-Words (BoW) strategy to represent SIFT features, as a histogram of visual codeword occurrences that represent an image. BoW can be summarised in three stages [32, 33, 19]: (i) Regions of 16×16 pixels over the image are used to represent the image as a set of feature vectors, in our case, using SIFT. (ii) Each feature vector is mapped to a certain codeword through a clustering process by K-Means algorithm. We set the number of codewords to 2000. (iii) The image is represented by calculating aggregated statistics of codewords, i.e. pooling. The pooling was done by applying Locally-Constrain Linear (LLC) [34] method with parameters $L = \{0, 1\}$. All parameters were experimentally obtained.

Finally, the feature vector of an image is formed by concatenating the considered global and local feature vectors, as explained above. Different combinations of feature vectors were tested, as shown in Section 4.

2.4. Char classification

Image classification is performed using two techniques, in Fig. 6: SVM [35] and deep learning [36] —in particular, Convolutional Neural Networks (CNN). The aim is to generate a model that predicts the char morphology group —low, medium or high reactivity.

2.4.1. SVM

SVM is a supervised training algorithm that learns a classification model from a set of feature vectors —training data— by choosing the best hyperplane that categorises new examples —in our work, char particle images. A good separation among classes —char morphology groups— is achieved by the hyperplane that has the largest distance to the nearest training data points of any class, see Fig. 6a. A regularisation parameter C controls the tradeoff between maximising the margin distance and minimising the training error. Based on several experiments, the parameter $C = 5$ led to the best result.

2.4.2. CNN

Hand-crafted features —e.g. global and local descriptors— may have a limited modelling and representational power to analyse complex natural images [37]. Instead, deep learning methods learn directly from the data at different levels of abstractions. CNN, an outstanding branch of deep learning applications to visual purposes, has shown record-shattering performances in a variety of computer vision problems, such as visual object recognition, detection and segmentation [38, 39, 40, 41]. The deeper the network, the more intricate structures it can understand. This hierarchy of abstraction is reached by stacking layers of "simple" functional modules [36]. From a visual point of view, the initial layers help in identifying low-level characteristics —e.g. points, edges, corners— while last layers contain more selective and semantic appreciations of the data —e.g. specific arrangements of the low-level features forming patterns or shapes— [42], see Fig. 6b. Similar to traditional approaches, features are extracted —using a set of filters present in convolutional layers— and then mined —through fully connected layers— to predict a suitable class for a given input image. It is important to remark that although the number of publications using CNN strategies has been increasing and the architectures getting more sophisticated in recent years, this is the first work using these tools for analysing char images to the best of the knowledge of the authors.

In practice, few CNN models are trained from scratch, since they require a significant amount of annotated data —which is scarce in most domains. Instead, transfer learning is used to adapt models trained on large datasets to a specified application. The main idea is to take advantage of well- and pre-trained networks by preparing them to work on a new domain. This choice presents two main advantages: (i) training takes less time in comparison to networks built from scratch, and (ii) deep architectures can be trained in small datasets. A conventional approach consists of using convolutional layers as feature extractors and modifying fully connected layers to fit the new problem. Naturally, the primary assumption is that the features calculated at training stage also describe image content on the new domain. In this work, two well-known proposals, VGG16 [43] and ResNet [39], were fine-tuned to classify char morphology groups. These networks have been selected since (i) they have achieved top performances in visual challenges, and (ii) their weights after training on massive collections of natural images are publicly available.

2.5. Coal characterisation

Characterisation of char particles is done using three reactivity levels: high, medium and low. A coal sample reactivity is inferred based on the relative frequencies of appearance of the three char groups. Finally, the char group with the highest rate indicates the reactivity of the coal sample.

3. Experimental Setup

We collected a dataset of 3661 char particle images as explained in Section 2.1 —where 1148, 1064 and 1448 images correspond to high, medium and low reactive groups, respectively. A random subset, 80% of the images, was used for training models; the rest was used for testing purposes. All images were manually labelled, i.e. assigned to one of the three char morphology groups, by experts. The labels of the training set were used to learn models whereas the ones of the test set were only used to evaluate the performance of the models on new images.

SVM classifiers were trained using 5-fold cross-validation. In this strategy, the training dataset was randomly split into five subsets of equal size, one subset was used for evaluation and the remaining ones for training the classifier. This process was repeated five times (the folds), i.e. each subset was used for evaluation. The classifier obtaining the highest accuracy measure during the cross-validation was selected for testing. In this work, we defined the accuracy measure as the percentage of particles correctly classified [44]. The accuracy values calculated for the test set are reported in Section 4.

The pre-trained VGG16 and ResNet models were adapted to the char domain using transfer learning. Both networks were trained at most for 50 epochs — i.e. the number of times the network sees the entire training dataset. The initial training set was randomly split into training and validation, 80% and 20% of the whole set respectively. While the former collection was used to fine-tune the network, the latter was used to monitor overfitting. In our case, the process was repeated until no improvement between consecutive epochs was observed. The model that obtained the highest accuracy on the validation set was kept and used for testing. Additionally, since results with original data were significantly low, data was augmented using Euclidean transformations (e.g. rotations, translations, scaling). All the deep learning experiments were run on a GNU/Linux machine box running Ubuntu 16.04, with 128GB RAM. CNN training and testing were carried out using a single GeForce GTX 1080 GPU (NVIDIA Corp., United States) with 12GB RAM.

4. Results and Discussion

4.1. SVM Results

We compared labels obtained automatically vs manually to calculate the accuracy. Table 3 presents the accuracy results using SVM classifiers trained with individual features —Global, LBP, HMCLOSIB, HOG and SIFT— for char images and their eight bit-plane slices. As it can be observed from the reported values, char slice images exhibit similar accuracy values in comparison to char images, in all cases.

Accuracy obtained by concatenating feature vectors on slice images are presented in Table 4. For each case, we show the difference between the accuracy with the baseline feature —i.e. feature vector extracted on the original char image— and the accuracy after concatenating feature vectors. Also, the performance of two classifiers using the relative change in accuracy is analysed. Given the accuracy values of two classifiers, A and B, the relative change in accuracy is defined as $RCA = ((A-B)/B)100$ —where a classifier A is trained with a set of proposed features, and a classifier B is trained with the baseline features. Positive values of RCA mean that A outperforms B. The higher the improvement in accuracy using proposed features, the better the out-performance of A compared to B. As it can be seen, feature concatenation led to accuracy improvement between 0.60% and 21.01%. The combination of global feature vectors calculated on slice images number 8 and 4 yielded an accuracy of 91.94%, but the improvement was minimal —0.60%. On the other hand, the concatenation of HMCLOSIB feature vectors computed on slices number 8, 4 and 1 exhibited an accuracy of 78.69% and obtained the maximum accuracy improvement —21.01%. These results may imply that merging information extracted from different slices helped in achieving a more detailed and meaningful description of char particles than standard char images.

We concatenated vectors of different features to find the best set of features to describe the char morphology groups. We found out that the best results were achieved by fusing the global feature vector calculated on the char image, global feature vectors extracted from slice images number 8 and 4, and also HMCLOSIB feature vectors obtained from slice images number 3 and 8. This classifier yielded an accuracy of 93.98%, an improvement of 2.83% compared to its baseline.

The analysis of one char particle took around 0.20 seconds using the baseline feature and an average of 0.70 seconds using the proposed concatenation of feature vectors, i.e. Global (Char image), Global (Slice 8, Slice 4) and HMCLOSIB

(Slice 3, Slice 8). The latter processing time corresponds to an increase of 3.6 times in comparison to the processing time of the Global (Char image) classifier. Besides, it should be noted that manual analysis requires in average between 7 and 37 seconds per char image depending on the operator's expertise [6]. Our method took less than one second to evaluate every char image. The processing time of the automatic classification of a char image was computed for the testing set —732 char images— using a laptop with a processor Intel Core i7 and 4GB of RAM.

4.2. Deep Learning Results

Table 5 presents the accuracy using deep learning models for the char images and their eight bit-plane slices. In this case, each slice image was replicated to obtain three channels that were passed to the network. Similarly to SVM, the use of bit-plane slices improved the results obtained when only the original char image was used.

Results of CNNs combining slice images to obtain a richer and more distinct representation of the char particles are shown in Table 6. Additionally, the difference of the accuracy and RCA between the performances of the baseline network —i.e. network built using the original char image— and the network using the combination of image slices is outlined. It is important to remark that two combination strategies were analysed: late and early fusion. The former consisted of merging predictions provided by networks trained on different image slices through majority voting. The latter contemplated concatenating three different slices to form the input of a single network. Results of this second approach are reported in Table 6. An improvement between 1.17% and 4.58% was observed using the concatenation of slice images instead of original char images. ResNet exhibited the minimum improvement —1.17%— with a classification accuracy of 82.92% using the image slices number 1, 2 and 8. VGG16 showed the maximum improvement —4.58%— with a classification accuracy of 84.15% using the image slices number 1, 2 and 3. When combining results of different networks, we found out that the best results were achieved by combining the networks ResNet (Slice 8), ResNet (Slice 1, Slice 2, Slice 8), VGG16 (Slice 1), VGG16 (Slice 2) and VGG16 (Slice 1, Slice 2, Slice 3). This classification model yielded an accuracy of 86.34%, which means an improvement of 5.33% w.r.t. ResNet(Char image). Nevertheless, the best classifier —accuracy of 93.98%— is obtained using SVM algorithm by concatenating Global (Char image), Global (Slice 8, Slice 4) and HMCLOSIB (Slice 3, Slice 8) feature vectors.

The training of each one of the networks took approximately 20 minutes. Once trained, models were able to produce classification results in less than 0.1 seconds. Majority voting was carried out offline (i.e. once the networks were fine-tuned) and it took less than 0.1 seconds to process. As expected, no particular variation regarding computational response was appreciated when computing information from a single slice or three at a time.

In general, classification models using deep learning approaches out-perform traditional supervised learning ones, such as SVM, in natural and medical image classification problems. But in this case, SVM models combining global and local features showed better classification results. One reason might be that the amount of annotated data available to tune the deep learning models is not enough to capture completely char image representation.

4.3. Results for Coal Characterisation

The ultimate aim of this work is to characterise the char during its combustion; this is to create an automatic system that efficiently estimates the percentage of char particles corresponding to each char morphology group in a sample of devolatilised coal by analysing a set of char particles. In this way, we used the char classification model obtained previously —with SVM and the concatenation of the feature vectors: Global (Char image), Global (Slice 8, Slice 4) and HMCLOSIB (Slice 3, Slice 8)— to analyse the reactivity of coal samples of three Colombian regions —Valle, Antioquia and Cundinamarca— by classifying 500 char particles per coal sample [7] generated at $900°C$ of temperate and $200ms$ of residence time.

In Table 7, we present the percentage of char particles that are classified in each char morphology group, both manually by experts and automatically using our proposal. Additionally, the percentage of char particles classified in the char morphology groups —high, medium and low reactivity— is computed. A non-zero value of the difference between manually and automatically classifications represents that these number of particles are miss-classified.

In particular, high reactive chars led to differences between 2.6% and −9.4%, medium reactive chars presented differences between 6.4% and −9.2%, and low reactive chars yielded differences between 1.8% and 3.8%. Those differences were caused by changes in image quality such as unfocused areas, as well as complexity in char shapes. Medium reactive chars tend to be misclassified as high or low reactive chars. However, the characterisation results were consistent with the manually obtained results. The char morphology group with the highest rate identified by our proposal correspond to the same group defined manually, in all cases. Recall that this char morphology group is commonly used as an estimation of coal reactivity.

The proposed approach allows to successfully classify char particles according to morphology and characterise coal sample reactivity in a fast and automatic way. In particular, coals from Cundinamarca produced char particles which are more reactive than char particles obtained from Valle and Antioquia coals.

5. Conclusion

Automatic systems can be built to characterise the morphology of chars generated during pulverised coal combustion. In this paper, we proposed a system to infer coal reactivity by classifying char particles into three char morphology groups —high, medium, and low char reactive. Char classification models were built using SVM and deep learning algorithms considering features obtained from char images and the eight bit-plane slices composing them. In particular, SVM models trained with global and local features allowed distinguishing better char particles into the char groups in comparison to models built using transfer learning on CNNs.

The proposed char classification system was validated by experiments using microscopy char images obtained from coals of three Colombia regions: Valle, Antioquia and Cundinamarca. Results showed that char image slices improved the accuracy of SVM and deep learning classification models in comparison to the classifiers built using only the original char image. Presumably, the reason is that image slices highlight relevant information that allows a better representation and classification of image content. Also, the proposed machine-vision approach is more than seven times faster than the traditional manual method and independent of the operator expertise.

The proposed approach is capable of estimating the coal reactivity of coal samples of the three Colombian regions by classifying 500 char particles per coal sample with small differences with respect to the char morphology groups manually defined. In particular, it was observed that coals from Cundinamarca produced char particles which were more reactive than char particles obtained from Valle and Antioquia coals. These results were consistent with manual analysis. Thus, we can say that our proposal can be used to characterise the reactivity of coal samples, with a precision similar to the obtained manually, but with the advantages of an automatic system that analyses char particles.

Acknowledgement

The scientific work was supported by COLCIENCIAS, Scholarship "Estudios de Doctorado en Colombia 2013 (Doctoral Studies in Colombia 2013)". Jose Bernal holds an FI-DGR2017 grant from the Catalan Government with reference numbers 2017FI B00476.

References

[1] J. Bailey, A. Tate, C. Diessel, T. Wall, A char morphology system with applications to coal combustion, Fuel 69 (2) (1990) 225–239.

[2] D. Vargas, D. Chaves, M. Trujillo, J. Pińeres, J. Barraza, Beneficiated coals' char morphology, Ingeniería e Investigación 33 (1) (2013) 13–17.

[3] A. Rojas, J. Barraza, Caracterización morfológica del carbonizado de carbones pulverizados: determinación experimental, Revista Facultad de Ingeniería Universidad de Antioquia 43 (2008) 42–58.

[4] S. Kzgut, M. Bilen, . Torolu, K. Bar, Size-related evaluation of unburned carbon, Combustion Science and Technology 188 (3) (2016) 439–450.

[5] D. Alvarez, E. Lester, Atlas of char occurrences. combustion working group, commission iii, in: Internacional Conference on Coal Petrology, ICCP, 2001.

[6] E. Lester, D. Alvarez, A. Borrego, B. Valentim, D. Flores, D. Clift, P. Rosenberg, B. Kwiecinska, R. Barranco, H. Petersen, M. Mastalerz, K. Milenkova, C. Panaitescu, M. Marques, A. Thompson, D. Watts, S. Hanson, G. Predeanu, M. Misz, T. Wu, The procedure used to develop a coal char classificationcommission {III} combustion working group of the international committee for coal and organic petrology, International Journal of Coal Geology 81 (4) (2010) 333 – 342.

[7] T. Wu, E. Lester, M. Cloke, Advanced automated char image analysis techniques, Energy & Fuels 20 (3) (2006) 1211–1219.

[8] A. Rojas, J.M.Barraza, Caracterización morfológica del carbonizado de carbones pulverizados: estado del arte, Revista Facultad de Ingeniería Universidad de Antioquia 41 (2007) 84–97.

[9] Alpana, S. Mohapatra, Machine learning approach for automated coal characterization using scanned electron microscopic images, Computers in Industry 75 (Supplement C) (2016) 35–45.

[10] Z. Zhang, J. Yang, Y. Wang, D. Dou, W. Xia, Ash content prediction of coarse coal by image analysis and ga-svm, Powder Technology 268 (Supplement C) (2014) 429 – 435.

[11] C. Igathinathane, U. Ulusoy, Machine vision methods based particle size distribution of ball- and gyro-milled lignite and hard coal, Powder Technology 297 (Supplement C) (2016) 71 – 80.

[12] D. Alvarez, A. Borrego, R. Menéndez, Unbiased methods for the morphological description of char structures, Fuel 76 (13) (1997) 1241 – 1248.

[13] M. Cloke, T. Wu, R. Barranco, E. Lester, Char characterisation and its application in a coal burnout model, Fuel 82 (1517) (2003) 1989– 2000.

[14] J. Reyes, Identificación de descriptores en imágenes de carbonizado, Master's thesis, Universidad del Valle (2009).

[15] D. Chaves, E. García, M. Trujillo, J. M. Barraza, Char morphology from coal blends using images analysis, in: World Conference on Carbon, CARBON, 2013, pp. 1–5.

[16] W. P. Adamczyk, A. Szlk, A. Klimanek, R. A. Biaecki, G. Wcel, A. Katelbach-Wozniak, S. Sadek, M. Ditaranto, N. E. L. Haugen, Visualization system for the measurement of size and sphericity of char particles under combustion conditions, Powder Technology 301 (Supplement C) (2016) 141–152.

[17] M. Schiemann, N. Vorobiev, V. Scherer, Stereoscopic pyrometer for char combustion characterization, Appl. Opt. 54 (5) (2015) 1097–1108.

[18] J. Riaza, J. Gibbins, H. Chalmers, Ignition and combustion of single particles of coal and biomass, Fuel 202 (Supplement C) (2017) 650–655.

[19] D. Chaves, M. Trujillo, J. Barraza, Global and local features for char image classification, in: Artificial Computation in Biology and Medicine, Vol. 9107 of Lecture Notes in Computer Science, Springer, Cham, 2015, pp. 98–107.

[20] A. O. C. Sáncheza, L. R. C. Riverac, J. D. J. D. Velásquezd, Análisis petrográfico de carbones colombianos mediante análisis de imágenes, in: III Congresso Brasileiro de Carvo Mineral, 2011, pp. 1–18.

[21] J. Cervantes, J. Taltempa, F. Garca-Lamont, J. S. R. Castilla, A. Y. Rendon, L. D. Jalili, Análisis comparativo de las técnicas utilizadas en un sistema de reconocimiento de hojas de planta, Revista Iberoamericana de Automática e Informática Industrial RIAI 14 (1) (2017) 104 –114.

[22] P. Matti, H. Abdenour, Z. Guoying, A. Timo, Computer Vision Using Local Binary Patterns, Springer, London Dordrecht, 2011.

[23] O. G.-O. Olivera, Methods for improving texture description by using statistical information extracted from the image gradient, Ph.D. thesis, University of Leon. Department of Electrical, System and Automatic Engineering (July 2017).

[24] N. Dalal, B. Triggs, Histograms of oriented gradients for human detection, in: Proceedings of the 2005 IEEE Computer Society Conference on Computer Vision and Pattern Recognition (CVPR'05) - Volume 1 - Volume 01, CVPR '05, IEEE Computer Society, 2005, pp. 886–893.

[25] D. G. Lowe, Object recognition from local scale-invariant features, in: Proceedings of the Seventh IEEE International Conference on Computer Vision, Vol. 2, 1999, pp. 1150–1157.

[26] R. C. Gonzalez, R. E. Woods, Image enhancement in the spatial domain, in: Digital Image Processing (2nd Edition), Pearson, 2002, Ch. 3, p. 86.

[27] G. Thomas, M. Annamalai, G. Karuppannan, Bit plane slicing technique to classify date varieties, Agricultural Engineering International: CIGR Journal 17 (2) (2015) 277–286.

[28] S. Thepade, R. Das, S. Ghosh, A novel feature extraction technique using binarization of bit planes for content based image classification, Journal of Engineering 2014 (2014) 1–11.

[29] T. Z. Lee, D. B. L. Bong, Analysis of bit-plane images by using principal component on face and palmprint database, Pertanika Journal Science & Technology 24 (1) (2016) 191–203.

[30] H. Wu, A. J. Pedersen, P. Glarborg, F. J. Frandsen, K. Dam-Johansen, B. Sander, Formation of fine particles in co-combustion of coal and solid recovered fuel in a pulverized coal-fired power station, Proceedings of the Combustion Institute 33 (2) (2011) 2845–2852.

[31] G. W. Zack, W. E. Rogers, S. A. Latt, Automatic measurement of sister chromatid exchange frequency., Journal of Histochemistry & Cytochemistry 25 (7) (1977) 741–53.

[32] G. Csurka, C. Bray, C. Dance, L. Fan, Visual categorization with bags of keypoints, Workshop on Statistical Learning in Computer Vision (2004) 1–22.

[33] S. Avila, N. Thome, M. Cord, E. Valle, A. d. A. Arajo, Bossa: Extended bow formalism for image classification, in: 2011 18th IEEE International Conference on ImageProcessing, 2011, pp. 2909–2912.

[34] J. Wang, J. Yang, K. Yu, F. Lv, T. Huang, Y. Gong, Locality-constrained linear coding for image classification, in: 2010 IEEE Computer Society Conference on Computer Vision and Pattern Recognition, 2010, pp. 3360–3367.

[35] B. E. Boser, I. M. Guyon, V. N. Vapnik, A training algorithm for optimal margin classifiers, in: Proceedings of the Fifth Annual Workshop on Computational Learning Theory, COLT '92, 1992, pp. 144–152.

[36] Y. Lecun, Y. Bengio, G. Hinton, Deep learning, Nature 521 (7553) (2015) 436–444.

[37] L. Deng, D. Yu, Deep learning: Methods and applications, Foundations and Trends in Signal Processing 7 (34) (2014) 197–387.

[38] A. Krizhevsky, I. Sutskever, G. E. Hinton, Imagenet classification with deep convolutional neural networks, in: Advances in neural information processing systems, 2012, pp. 1097–1105.

[39] K. He, X. Zhang, S. Ren, J. Sun, Deep residual learning for image recognition, in: Proceedings of the IEEE conference on computer vision and pattern recognition, 2016, pp. 770–778.

[40] C. Szegedy, S. Ioffe, V. Vanhoucke, A. A. Alemi, Inception-v4, inception-resnet and the impact of residual connections on learning., in: AAAI, 2017, pp. 4278–4284.

[41] H. Noh, S. Hong, B. Han, Learning deconvolution network for semantic segmentation, in: Proceedings of the IEEE International Conference on Computer Vision, 2015, pp. 1520–1528.

[42] L. Deng, A tutorial survey of architectures, algorithms, and applications for deep learning, APSIPA Transactions on Signal and Information Processing 3 (2014) e2.

[43] K. Simonyan, A. Zisserman, Very deep convolutional networks for large-scale image recognition, CoRR abs/1409.1556.

[44] D. M. Powers, Evaluation: from precision, recall and f-measure to roc, informedness, markedness and correlation, Journal of Machine Learning Technologies 2 (1) (2011) 37–63.

Figures

Figure 1: Stages of the proposed char characterisation system. a) Acquisition of input char images from a char-block. b) Image preprocessing by removing the background (char-block resin) and calculating bit-plane image slice. c) Feature extraction of global and local features to describe the particles and generate a feature vector. d) Particle classification using supervised learning into high, medium or low reactive morphology groups. e) Coal characterisation by calculating the percentages of particles that belong to each char morphology group. In this example, the coal is characterised as high reactive.

Figure 2: Laboratory equipment used to simulate coal devolatilisation and generate char particles.

Figure 3: Image acquisition process. In d) resin is seen as quite uniform grey background and chars are seen as white or grey particles.

Figure 4: Background removal of a char particle image using the Triangle method. For this specific char image sample, $t = 111$.

Figure 5: Illustration of bit-plane slicing decomposition of a char particle image.

Figure 6: High level illustration of the classification algorithms. a) SVM. b) Deep learning network.

Tables

Table 1: Description of char types in the ICCP classification and char groups considered in this work.

Char type	Char image	Description	Char morphology group
Tenuisphere, TS	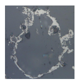	Shape appears spherical with angular roundness. Porosity rate is above 80%, majority of wall thickness measures 3μm or less. Fuse material presence is larger than 75%.	High Reactive
Crassisphere, CS	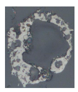	Shape appears spherical with angular roundness. Porosity rate is above 60%, majority of wall thickness measures 3μm or less. Fuse material presence is larger than 75%.	
Tenuinetwork, TN	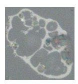	Internal structure appears like a network. Porosity rate is above 70%, majority of wall thickness measures 3μm or more. Fuse material presence is higher than 75%.	
Crassinetwork, CN	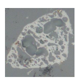	Internal structure appears like a network. Porosity rate between $40-70\%$, majority of wall thickness measures 3μm or less. Fuse material presence is higher than 75%.	
Mixed Porous, MP	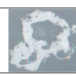	Unfused material rate within $25-75\%$. Porosity proportion above 60%.	Medium Reactive
Mixed Dense, MD	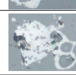	Unfused material rate within $25-75\%$. Porosity proportion within $40-60\%$.	
Inertoid, I	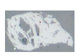	Dense. Porosity rate within $5-40\%$. majority of wall thickness measures 3μm or less. Presence of both fused and unfused material.	Low Reactive
Solid, S		Solid appearance. Porosity rate less than 5%. Unfuse material presence is higher than 75%.	
Mineroid	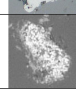	Particle with predominant inorganic matter.	—

Table 2: Description of morphological global features.

Global feature	Illustration	Description
Area		Total number of white pixels on the binary image obtained after thresholding.
Devolatilised material	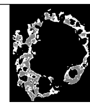	Grey intensities in char images with values between 160 and 255 approximately.
Undevolatilised material	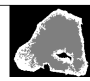	Grey intensities in char images with values between 130 and 160 approximate.
Number of pores		Count of identified voids (pores) of a particle.
Porosity	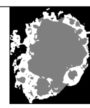	Ratio between pore and particle areas.
Sphericity	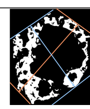	Ratio between the minimum and the maximum Feret diameter of the particle.
Wall thickness	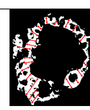	Line transects are used for calculating wall thickness. The first, second and third quartile of wall thickness distribution. are computed

Table 3: Accuracy values of SVM models trained with Global, LBP, HMCLOSIB, HOG and SIFT features calculated with original images and their eight slices. The best accuracy values are highlighted in bold.

Feature	Char image	Image slice 1	2	3	4	5	6	7	8
Global	**91,39**	75,00	78,55	78,68	76,36	71,72	68,44	62,02	91,12
LBP	78,96	77,04	76,36	76,91	73,90	68,85	67,75	64,89	**79,09**
HMCLOSIB	65,02	**75,95**	74,31	75,13	70,35	62,02	61,06	58,60	67,75
HOG	60,79	63,25	**64,75**	63,93	61,20	59,97	61,88	61,61	62,29
SIFT, $L = 0$	**80,46**	76,50	72,13	73,08	74,04	67,62	66,66	63,79	79,50
SIFT, $L = 1$	**83,74**	83,06	79,64	79,50	79,78	76,91	74,45	68,98	83,06

Table 4: Accuracy values obtained with SVM classifiers using concatenations of features extracted from original and bit-plane slice images. The two last columns indicate the difference and improvement between the proposed features and the baseline features, respectively. Higher positive values mean a better performance. The best accuracy value in each case is presented in bold.

Feature (considered images)	Accuracy	Diff vs Baseline feature	RCA
Global (Char image) —*Baseline*—	91.39	—	—
Global (Slice 8)	91.12	-0.27	-0.30
Global (Slice 8, Slice 3)	92.35	0.96	1.06
Global (Slice 8, Slice 4)	91.94	0.55	0.60
Global (Slice 8, Slice 4, Slice 3, Slice 1)	**92.49**	**1.09**	**1.20**
HMCLOSIB (Char image) —*Baseline*—	65.03	—	—
HMCLOSIB (Slice 1)	75.96	10.93	16.81
HMCLOSIB (Slice 8, Slice 1)	77.46	12.43	19.12
HMCLOSIB (Slice 8, Slice 3)	76.78	11.75	18.07
HMCLOSIB (Slice 8, Slice 4, Slice 1)	**78.69**	**13.66**	**21.01**
LBP (Char image) —*Baseline*—	78.96	—	—
LBP (Slice 8)	79.10	0.14	0.17
LBP (Slice 8, Slice 3)	80.19	1.23	1.56
LBP (Slice 8, Slice 4)	80.33	1.37	1.73
LBP (Slice 8, Slice 4, Slice 3)	**80.74**	**1.78**	**2.23**
HOG (Char image) —*Baseline*—	60.79	—	—
HOG (Slice 2)	64.75	03.96	6.52
HOG (Slice 3, Slice 2)	63.25	2.46	4.04
HOG (Slice 6, Slice 2)	**63.52**	**2.73**	**4.49**
HOG (Slice 6, Slice 2, Slice 1)	62.02	01.23	2.02
SIFT, $L = 0$ (Char image) —*Baseline*—	80.46	—	—
SIFT, $L = 0$ (Slice 8)	79.51	-0.96	-1.19
SIFT, $L = 0$ (Slice 8, Slice 1)	**82.38**	**1.91**	**2.38**
SIFT, $L = 0$ (Slice 8, Slice 4)	81.28	0.82	1.02
SIFT, $L = 0$ (Slice 8, Slice 2, Slice 1)	81.97	1.50	1.87
SIFT, $L = 1$ (Char image) —*Baseline*—	83.74	—	—
SIFT, $L = 1$ (Slice 8)	83.06	-0.68	-0.82
SIFT, $L = 1$ (Slice 8, Slice 4)	84.84	1.09	1.30
SIFT, $L = 1$ (Slice 3, Slice 1)	84.56	0.82	0.98
SIFT, $L = 1$ (Slice 8, Slice 4, Slice 1)	**85.52**	**1.78**	**2.12**
[Global(Char image), Global (Slice 8, Slice 4), HMCLOSIB (Slice 3, Slice 8)]	**93.98**	—	—

Table 5: Accuracy results obtained with deep learning models using original images and their eight slices. The best accuracy values are highlighted in bold.

Network architecture	Char image	Image slice							
		1	2	3	4	5	6	7	8
VGG16	81.96	82.37	81.96	81.55	80.87	74.72	77.18	72.95	**82.92**
ResNet	80.46	**83.06**	82.10	81.01	77.73	79.50	73.63	73.63	81.42

Table 6: Accuracy values obtained with deep learning classifiers using feature combinations from original images and eight slices. The two last columns indicate the difference and improvement between the proposed features and the baseline features, respectively. Higher positive values mean a better performance. The best accuracy value in each case is presented in bold.

Network architecture (Images used)	Accuracy	Diff vs Baseline network	RCA
VGG16 (Char image) —*Baseline*—	80.46	—	—
VGG16 (Slice 2)	83.61	3.14	3.90
VGG16 (Slice 1, Slice 2, Slice 3)	**84.15**	**3.69**	**4.58**
ResNet (Char image) —*Baseline*—	81.97	—	—
ResNet (Slice 8)	**82.92**	**0.96**	**1.17**
ResNet (Slice 1, Slice 2, Slice 8)	82.92	0.96	1.17
[ResNet (Slice 8), ResNet (Slice 1, Slice 2, Slice 8), VGG16 (Slice 1, Slice 2, Slice 3), VGG16 (Slice 1), VGG16 (Slice 2)]	**86.34**	—	—

Table 7: Percentages of char particles per morphological group using manual and automatic classification. Diff vs Manual column indicates the difference between the automatically and the manual classification, as an error estimation. The closer the values to zero, the lower the classification error.

Char morphology	Coal from Valle			Coal from Antioquia			Coal from Cundinamarca		
	Manual	Automatic	Diff vs Manual	Manual	Automatic	Diff vs Manual	Manual	Automatic	Diff vs Manual
High reactivity	52.80	58.20	5.40	27.00	29.60	2.60	63.00	53.60	-9.40
Medium reactivity	16.00	6.80	-9.20	41.00	36.60	-4.40	20.00	26.40	6.4
Low reactivity	31.20	35.00	3.80	32.00	33.80	1.80	17.00	20.00	3.00